IOSR Journal of Electronics and Communication Engineering (IOSR-JECE)
e-ISSN: 2278-2834,p- ISSN: 2278-8735.Volume 11, Issue 1, Ver. IV (Jan. - Feb .2016), PP 37-44
www.iosrjournals.org

Determination of Dice Coefficient of Diseased Renal Images

R. Gomalavalli [1], S. Muttan[1] P. M. Venkatasai[2]
[1]*Department of Electronics and Communication Engineering, College of Engineering Anna University, Chennai, India*
[2]*Department of Radiology, Sri Ramachandra Medical College, Chennai, India*

Abstract: *In this paper, an effective method for computer-assisted renal segmentation of abdominal Computed Tomography (ACT) images with anatomic structure consideration is presented. The proposed segmentation system is expected to assist medical practioners in treatment planning, diagnosis and learning methodology. The planned method is a common to sound segmentation of two stages. First of all, the subject renal region is mined according to the statistical geometric location of renal. This method is applicable to images of different sizes (512 x 512) by using the statistical distance of the renal region. The Morphological operation process is the second stage of the renal segmentation. The main elements of the proposed system are: (i) the spine location is considered as the reference landmark for the renal region coordinates; (ii) Eroded the neighboring organs and selection of renal regions; (iii) directional removal of line connecting two regions on the consecutive ACT images is used for both (left &right) renal object detection in a time and (iv) Evaluation of DSC(Sorensen Dice Similarity Coefficient < 1) is done. In addition, Implementation of a visualization tool will automatically show the object detection for the physicians in different views. Renal regions from ACT images contain different pathologies in clinical practices and segmentation is must. The test series result on 242 images from 42 patients indicates a typical correlation coefficient of up to 94% between manual and automatic segmentation.*

Keywords*: Abdominal ACT images, renal image segmentation, renal object detection, morphological operations.*

I. Introduction

Image segmentation is one of the most significant issues in clinical practice. It is used in the analysis, monitoring and diagnosis of numerous applications such as to measure the tissue volumes, have the study of anatomical structure, localization of tumor and pathology, treatment planning, and Intra-surgery navigation [1]. There are two main reasons for the use of computer assisted segmentation: one is to improve upon the predictable user guided segmentation [2], and the other one is to acquire segmentation prior to revelation or visualization for the analysis of medical images [3]. Recently many computer-assisted diagnostic systems have been extended to assist in the making of precise and objective diagnoses for renal mascus, renal cyst, renal cancer and pyelonephritis. However, reasonably a little research has been directed on renal segmentation. End of a literature survey, we decided to do renal segmentation analysis in two category. One is Morphological operations of Blob Detection and region growing method of Boundary Detection.Daw-Tung Lin and Siu -Wan Hung proposed an effective method of model based approach of computer–aided kidney segmentation of abdominal CT images with anatomic structure [1]. Qingsong Zhu and Zhan song proposed a segmentation method of video with dynamic block diagram has been an importance research topic in intelligent surveillance and human-machine interface technologies [2]. Kang and Yang performed a approach of colour images are due to the grey level [3]. Zhang proposed a method Based on image segmentation evaluation techniques [4].

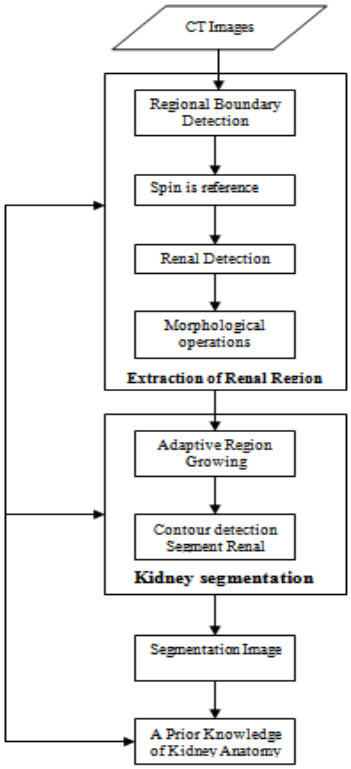

Fig. 1. Flowchart of the proposed renal segmentation system

Kobashi and Shapiro described a knowledge-based procedure for identifying and extracting organs from normal CT imagery [5]. Kobashi and Shapiro described a knowledge-based procedure for identifying and extracting organs from normal CT imagery [5]. The detection result was rated 85% grade A from testing of 75 images from three patients. Tsagaan and Shimizu proposed a deformable model approach for automatic renal segmentation [13]. They used a deformable model represented by the grey level appearance of renal and its statistical information of the shape. They tested 33 abdominal ACT images. The degree of regularity between automatic segmentation and manual positioning was 86.9%.

The main objective of this work is to develop an automatic renal segmentation of abdominal ACT images by combining the morphological operations and region growing method. Prior knowledge regarding anatomy and image processing techniques has been incorporated. The major features of the proposed system **:** **(**i) the spine location is considered as the reference landmark for the renal region coordinates; (ii) Eroded the neighboring organs and selection of renal regions; (iii) directional removal of line connecting two regions on the consecutive ACT images is used for object detection (iv)Evaluation of DSC(Sorensen Dice Similarity Coefficient)<1 and 5) region growing is controlled by the property of image homogeneity. The flowchart of the proposed automatic renal segmentation system is illustrated in **Fig.1**.

II. Materials And Method

2. Mining of the Subject Renal Region

A typical abdominal ACT image is very complicated. It may contain many neighboring organs like renal, liver, spleen, spine, fat, and pathologies. To achieve the goal of automatic renal segmentation, we proposed a common to well approach methodology. The abdominal cavity is first defined by an abdominal cavity boundary shape detection algorithm. Based on this shape, the spine location is marked as reference, and the subject renal regions (SRr) recognized accordingly. Since the slice thickness for ACT scanning and machine settings might differ from hospital to hospital, from machine to machine and from patient to patient. The middle slice of the sequence in which the renal is usually lucid and simple to interpret and analyze. Usually in the ACT images the abdominal cavity renal outer boundary is usually a bright line (dark area) formed by the X-ray reflection from skin. Thus, the outer-boundary area is determined by justifying whether there are dark pixels on the opposite sides in two directions. It is possible to discard small threads inside the boundary. However, the main purpose is to delineate the boundary, the inside area will be retained for the next stage. The boundary detection algorithm is shown as follows.

2.1. Abdominal Cavity Boundary Detection Algorithm:

```
[B,L,N,A]=bwboundaries (output);
hold on;
for k=1:length(output),
if(~sum(A(k,:)))
boundary = B{k};
for l=find(A(:,k))'
boundary = B{l};
```

In the CT image, all pixel values are represented as U(P,Q) where x and y are two coordinates and initially set position up = false, position down = false , position left = false, position right = false

for K = 1 to 4

position up = true, if U (P+ K, Q) ≤ 2

position down = true, if U (P − K, Q) ≤ 2

For L=2,

Position left= true, if U (P, Q + L) ≤ 2

Position right=true, if U (P,Q − L) ≤ 2

If both position up = 0 and position down = 0 then set U (P,Q)= 0

If both position left = 0 and position right = 0 then set U(P,Q) = 0

End

The spine location is considered as the reference landmark for the renal region coordinates and used to determine the position of renal regions. Consider the length of horizontal axis and the length of vertical axis as h, v respectively.

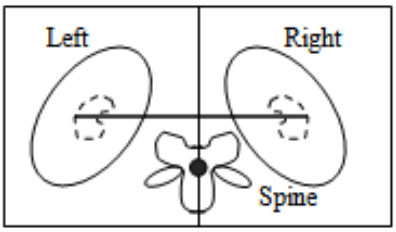

Fig.2. Subject Renal Region (SRr) is indicated in dotted lines

The spine, denoted as "Z" in **Fig. 2**, is located at position (0.5*h*, 0.53v). The subject Renal region (*SRr*) is then obtained by rotating a designed ellipse with a short axis length of 0.67hand long axis length of 0.33v. The center (p_0, q_0) of the initial ellipse is located at a distance of (0.3*h*) to the spine. Generally, both renal appear in an angle of inclination in the range of 40◦–80◦. The heuristic for choosing relative distances, locations, and revolution is based on the estimation after analyzing 80 images and refers to Tsaggaan's report [13].

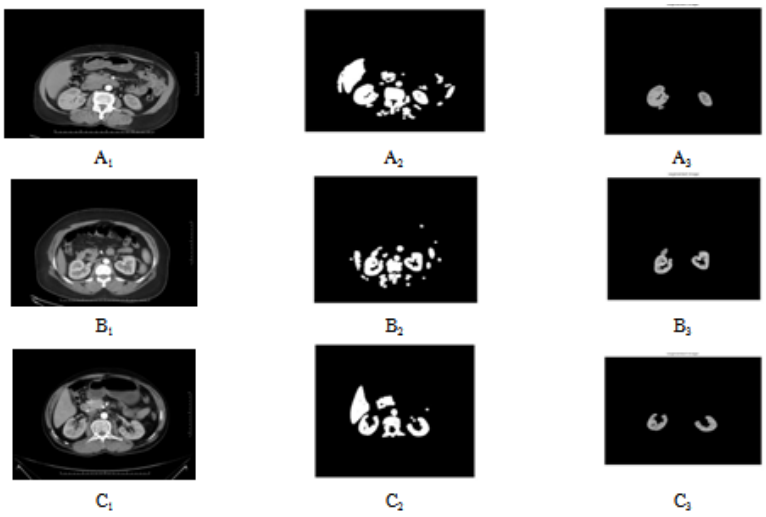

Fig.3. Extraction of Renal Region with best approach versus. Renal Images (A_1, B_1, C_1).Morphological operation images (A_2, B_2, C_2). Segmentation Image (A_3, B_3, C_3).

Thus, a more reliable *SRr region* is obtained by rotating the preliminary pixel U (p,q) in the *SRr* according to the geometric transformation (60 degree for left renal, 60 degree for right renal) [7]. Using

the rotated disc subject renal regions is more suitable, because they regularly contain the renal compared to the morphological operation method. We examined 80 training images, and it is apparent that the planned segmentation approach is consistent. The rates of complete renal coverage by using our method and using the morphological method are 97.6% and 95%, respectively. Three results of renal region extraction are shown in **Fig. 3 (A_2, B_2, C_2).** During detection stages discarded the spike-like noises using median filter [7] and some of the pixels are replaced by zero values inside the boundary.

Renal Image Segmentation

After the subject renal region has been extracted, started to regain the renal from the *SRr*. Region growing, labelling, filling, erosion and dilation as well as mathematical morphology are used for the image processing techniques.

Adaptive Region Growing:

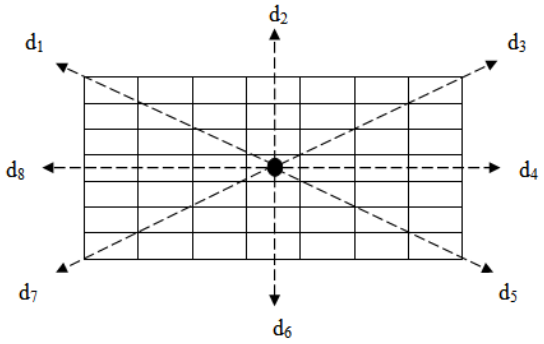

Fig. 4. Initial seed Direction Model.

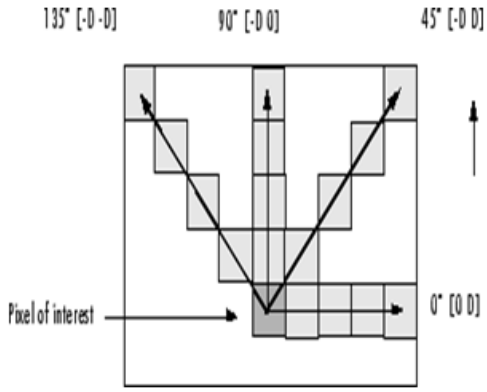

Fig. 5. Direction of pixel interest

Region growing process is under three step: (1) Initialization of seed points (2) similarity condition of region growing and (3) and the termination condition. An adaptive region growing condition by constructing a model of eight search directions (**see Fig. 4 & Fig. 5**) in terms of local frequency inside the SRr. Since the renal is identical area, we estimate the difference of grey levels between the maximum and minimum pixel values in a 7 X 7 mesh.

Initially ‘θ ‘as threshold for 20,if (max-min) > θ, then the center of mesh sited in a non-identical area and it is not correct to be an initial seed of renal area. Simplification is preserved through the normalization process of 80 training images in which the grey level of subject renal region images were adjusted to the corresponding mean values (104 and 111). The deviation of mean values is due to the enhancement of contrast medium and the nature of different anatomic structure of the two renal region. The search procedure is continued until the entire SRr has been tested. Threshold value θ is adjusted for the contrast variance. Slowly the threshold range is adjusted from 5 to 40 in order to provide a normal renal region. We will now propose a more prescribed formulation of this approach.

3.1.1. Seed Point selection:

First, we suggest the (pi, qj) is the initial seed point location of the renal regions .Let the centre slice index C = ((pi+qj)/2), where pi, qj is the distance point of seed point. Let max and min denote the maximum and minimum intensity in a 7X7 mesh, respectively [7 X 7]. The mesh is centered on the seed coordinates (pi, qi). The algorithm is shown as follows.

Seed Point Selection Algorithm*:*
Set ρ = 0.3t, where t = slice thickness of the scan (8–10 mm) and based the selection of 80 abnormal images [13], [8]. Let max and min denote the maximum and minimum intensity in a 7 X7 mesh, respectively. The mesh is centered on the seed coordinates (pi,qi).
for image slice i =1to n
compute the initial seed location (xi ,y i)and ρ =0.3t
pi = x0 −ρ(i −C) for left K_L
pi = x0 + ρ(i −C) for right K_R
qi = y0 −ρ(i −C) for direction d1 to d8 (depicted in **Fig. 4**),
move one pixel forward iteratively
if (max −min) ≤ θ1
then (pi ,qi) is identified as the center seed point,
and terminate
otherwise continue
if no seed point is found, then θ1 +5
if θ1 > 50 terminate end

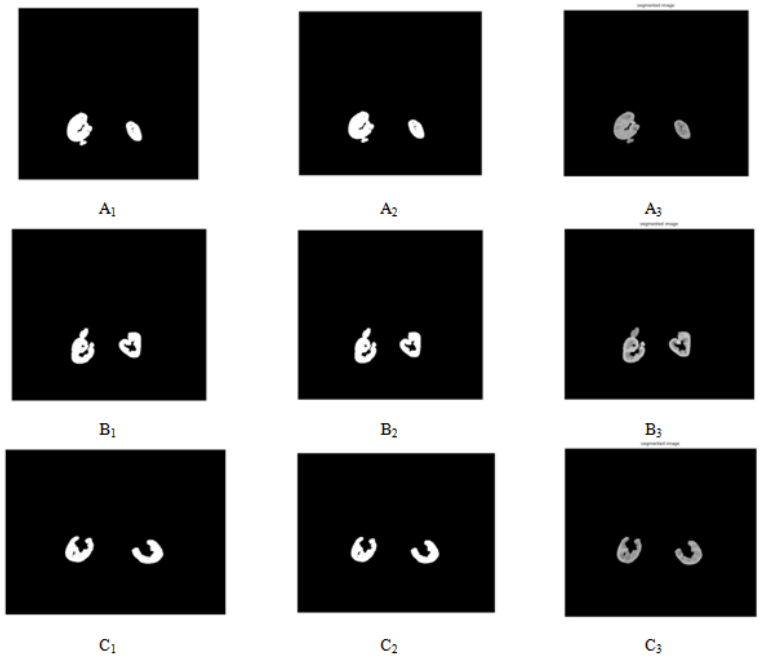

Fig. 6. Renal Region sequences for Segmentation of different Diseased cases Morphology Result(A_1, B_1, C_1), Binary Image (A_2, B_2, C_2), Final Segmentation (A_3, B_3, C_3).

We used multistage mathematical morphology operation to reduce the scattered pixels and detect the kidney object. Multistage mathematical morphology is a powerful tool in image processing. Morphological operation, such as erosion, dilation etc., are used for extracting, modifying, manipulating the features present in the image based structure element. The automatic Segmentation of different diseased Renal region subject sequences is proposed in **Fig.6**.

3.1.2. Renal Region Growing Criterion:

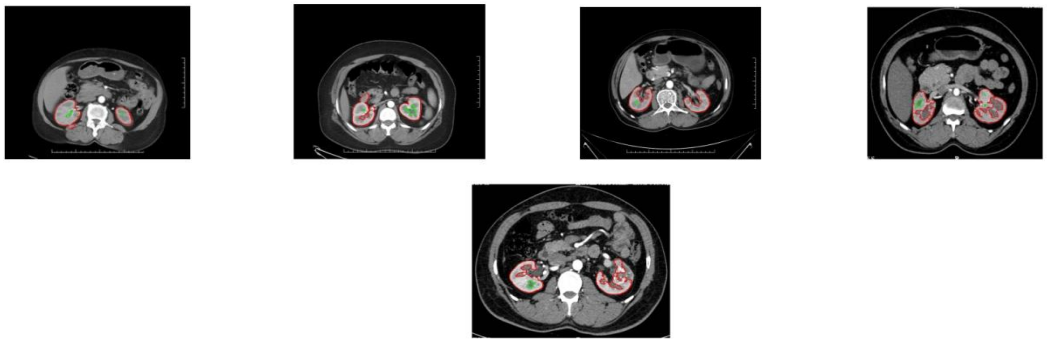

Fig.7. Boundary Detection of Renal Region Growing

Region growing is an approach in which the neighboring pixels are examined end added to a region class if no edges are detected. Indicate the initial seed point selection starts at (pi, qi).The consistent criterion is destined to $|U(p, q)-M0| \leq C$, $\forall (p, q) \in SRr$, where U(p, q) is a pixel satisfying the 8-connection condition around the seed, $M_0 = (max + min)/2$, where max and min indicates the maximum and minimum intensity of the mesh centered at U(p, q) *C* represents the contrast range of the initial seed (pi, qi). The Boundary detection of diseased Renal regions are exposed in **Fig.7** .Termination of region growing criterion is obtained when the area is heterogeneous. Appearance of the pathologies in the renal region give rise to weak seed points in selection and based on the investigation the threshold value is greater than 50.

3.2. Contour Detection:

Binary image is obtained from the region growing method is irregular and gap is found inside the renal object. Region growing is vital for image segmentation in which neighboring pixels are examined and added to a region class if no edges are detected. Adjustment has to be done to get better segmentation accuracy. The variation in accuracy may occur due to blood flow, image intensity and timing of scanning. Segmentation accuracy is improved by pixel filling, erosion, dilation and labelling method. Point –to –point technique is used to fill the gap in the segmented objects. Some of the morphological fundamentals are used for the renal region gap modification done by using the erosion, dilation and labelling the algorithm.

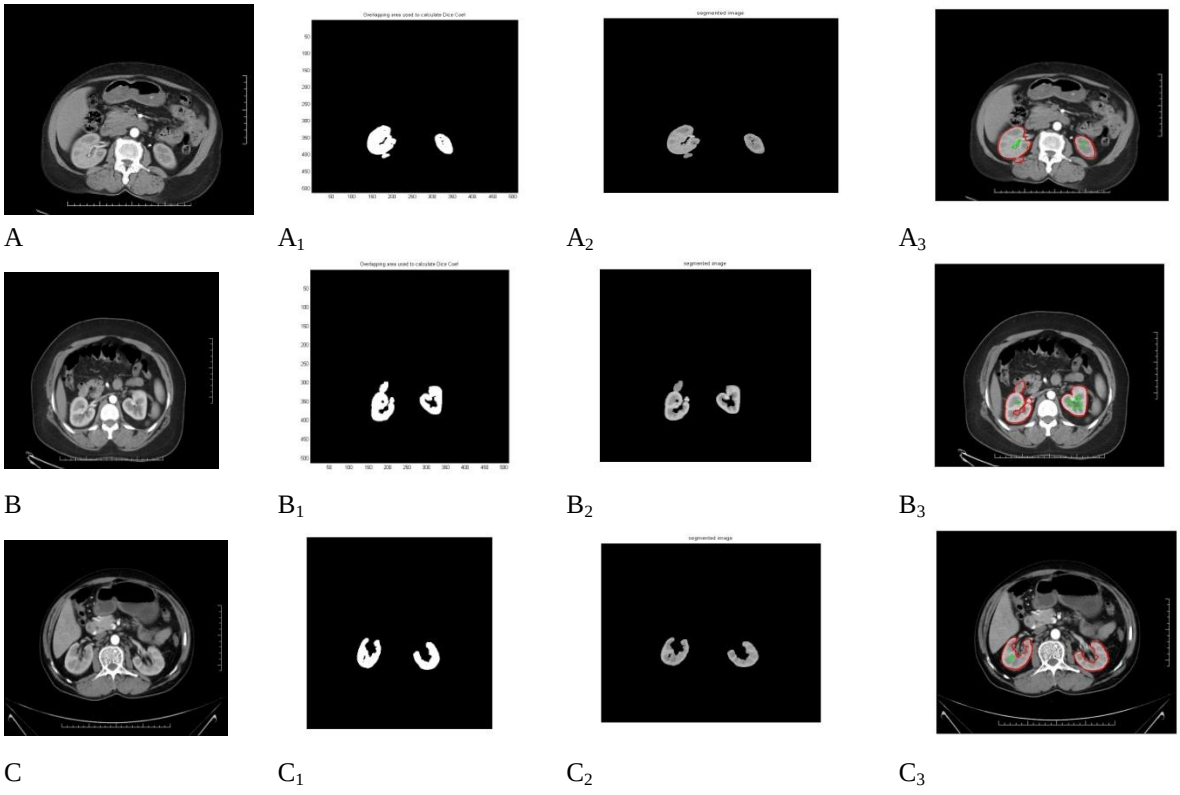

A A_1 A_2 A_3

B B_1 B_2 B_3

C C_1 C_2 C_3

Fig. 8 Interfacing Implementation of Renal Segmentation (A, B, C), Overlapping Area (A_1, B_1, C_1), Segmentation image (A_2, B_2, C_2), Boundary Detection (A_3, B_3, C_3).

Binary image has been obtained from the adaptive region growing process, trivial and irregular objects may remain and holes may scatter inside the organ. Region modification is important to improve the segmentation accuracy under various conditions arising from clinical practices such as the timing and rate of contrast media injection, image intensity variations, and blood flow rate. We have implemented the region modification by utilizing a series of image processing skills including: pixel filling, morphological operation (erosion, labeling, and dilation) [6]. To identify the irregular objects inside the renal region, an efficient filling algorithm is proposed which is modified from the seed point containment technique .Once the erosion operation is applied; renal region is separated into two or more sub-regions. The labeling operation is provided to discard the neighboring organ except the renal region by directional view. After this, dilation is provide to fulfill the eroded region with pixels of same structuring elements

III. Experimental Results

The renal ACT data used in this study was acquired from three CT scanners, HiSpeed LX/i by GE, and PQ2000 by Packer. The types of pathology meet in the abnormal scans include: renal mascus, renal cyst, renal cancer pyelonephritis. The abnormality images taken for analysis are 10 in above mentioned each case and 100 normal images for feature extraction. The proposed system was applied to segment the renal contours on 242 CT images. Usually, most physicians make their diagnosis of the ACT images by direct observation. The segmentation accuracy of the extracted region by the proposed approach is evaluated by two criteria. The criterion is a statistical validation of image segmentation quantitative indexes based on a spatial overlap correspondence (Sorensen Dice similarity coefficients) [1], Jaccard Coefficient and Jaccard Distance. The correlation between the automatic segmented region and the manual segmented one is calculated. The higher the value the higher the accuracy of the segmentation. The higher accuracy is obtained for the non-neighboring intersection organs. The Renal subject interfacing implementation is illustrated in **Fig.8.**

Table I Statistical Evaluation: Measured By The Sorensen Dice Similarity Coefficient(Sdsc), Jaccard Coefficient, Jaccard Distance & Mean

ACT Images	SE000	SE001	SE002	SE003	Average	Worst	Best
SDSC	0.9680	0.9766	0.9687	0.9520	0.9711	0.9520	0.9766
Jaccard Coefficient	0.8669	0.9001	0.8899	0.8281	0.8712	0.8281	0.9001
Jaccard Distance	0.1331	0.0999	0.1101	0.1101	0.1133	0.1101	0.0999
Mean	120	122	121	121	121	121	122

Table Ii Qualitative Performance Of 42 Patients

Segmentation	Comparable(A) %	Acceptable(B) %	Not Acceptable(C) %
Manual	68.3	29.3	2.4
Automatic	68.9	29.5	1.6
Average	68.6	29.4	2.0

A B C D E

Examples of manual segmentation are shown in Fig. 8(a).

A_1 B_1 C_1 D_1 E_1

Examples of Automatic segmentation are shown in Fig. 8(b).

The statistical Evaluation of image quality segmentation is measured by Sorensen Dice Similarity Coefficient $I(A1, A2) = (A1 \cap A2)/(A1 \cup A2)$ between the automatic segmented region ($A1$) and the manual segmented region ($A2$) **[7].** Manual segmentation were performed for all scans by a radiologist who carefully pointed out the boundaries of the renal region using a computer mouse is shown in **Figure 8(a).** The amount of average overlap for all the scans (242 images) is shown in **Table I** typically, the proposed automatic segmentation achieved 0.90 correlation with the manual segmentation is average. The best segmentation is 0.978, which means the result of the automatic segmentation is almost the same as that of manual segmentation. The worst segmentation is 0.952. These statistics indicate that the performance evaluations show a satisfactory segmentation result. During segmentation the quality statistical evaluation is very low due to neighboring organs interaction. Examples of Automatic segmentation ae shown in **Fig.8(b).**The cortex thickness is very low range for the diseased delineation images.

For a better qualitative Analysis comparison is made between manual and automatic segmentation of renal regions which gives 98.2% of acceptable performance. The average performance is 1.9%.Three Category of Qualitative analysis is made of comparable (A), acceptable (B) and not acceptable(C). The qualitative performance is shown in **Table II.**

IV. Conclusion

An expert method combining the aspects of anatomic structure of image processing techniques has been planned for renal segmentation of abdominal ACT images. First of all, the subject renal region is mined according to the statistical geometrical location of renal and a priori anatomical knowledge of the renal. This approach is applicable to images by applying relative distance of the renal region to the spine "Z". Furthermore, we proposed a disk candidate renal region extraction approach with progressive positioning for the center of disk on the consecutive ACT images. This way, the planned renal regions selection method becomes more consistent than the fixed area method proposed by Tsagaan, *et al.* This paper originality lies in the preprocessing step, which deliberates anatomic landmarks and measures to define a disk initial search region. Next, we extended a morphological operation region growing for renal segmentation and provided a contour detection approach so as to achieve an accurate renal extraction is shown in figure 8(b). We applied the planned method to 242 images from 42 patients with pathologies and evaluated the segmentation performance qualitatively and quantitatively. The test series result on 242 images from 42 patients indicates a typical correlation coefficient of up to 94% between manual and automatic segmentation. However, more work is essential to verify the technique on a better and more diverse dataset

Acknowledgment

The authors would like to thank Hoc of Department of Radiology, Sri Ramachandra University for his help in image collection and performing manual segmentations. Acknowledgement also to Dr.S. Siva priya, M.D for guidance of images evaluation and precious suggestions.

References

[1]. Automated detection of nodules in peripheral lung fields," Med. Phys., vol. 15, no. 2, pp. 158 – 166, 1988.
[2]. M. Kobashi and L. G. Shapiro, "Knowledge-based organ identification from CT images," Pattern Recogn., vol. 28, pp. 475–491, 1995.
[3]. Zhang, Y. J., 1997. Evaluation and comparison of Different segmentation algorithms. Pattern Recognition Letters, 18(10). Pp. 963-974
[4]. J. R. Parker, Algorithms for Image Processing and Computer Vision. New York: Wiley, 1998
[5]. J. Fan, D. K. Y. Yau, A. K. Elmagarmid, and W. G. Aref, "Automatic image segmentation by integrating color-edge extraction and seeded region growing," IEEE Trans. Image Process., vol. 10, no. 10, pp. 1454– 1466, Oct. 2001.
[6]. R. Pohle and K. D. Toennies, "Segmentation of medical images using adaptive region growing," in Proc. Int. Soc. Opt. Eng. (SPIE), vol. 4322, 2001, pp. 1337–1346.
[7]. R. Pohle and K. D. Toennies, "A new approach for model-based adaptive region growing in medical image analysis," in the 9th Int. Conf. Computer Analysis of Images and Patterns, vol. 2124, Warsaw, Poland, 2001, pp. 242–246.
[8]. "Self-learning model-based segmentation of medical images,"Image Process. Commun., vol. 7, pp. 97–113, 2001
[9]. R. C. Gonzalea and R. E. Woods, Digital Image Processing, 2nd ed., Reading, MA: Addision-Wesley, 2002.
[10]. B. Tsagaan, A. Shimizu, H. Kobatake, and K. Miyakawa, "An automated segmentation method of renal using statistical information," in Proc. Medical Image Computing and Computer Assisted Intervention, vol. 1, 2002, pp. 556–563.
[11]. B. Tsagaan, A. Shimizu, H. Kobatake, and K. Miyakawa, "Development of extraction method of renals from abdominal CT images using a three- dimensional deformable model," Syst. Comput. Jpn., vol. 34, pp. 37–46, 2003.
[12]. X. Wang, L. He, and W. G. Wee, "Deformable contour method: A constrained optimization approach," Int. J. Comput. Vision, vol. 59, no. 1, pp. 87–108, 2004.
[13]. M. L. Giger, K. Doi, H. Mac Mahon, C. E. Metz,and F. F. Yin, "Image feature analysis and computer-aided diagnosis in digital radiography.
[14]. Daw-Tung Lin, Member, IEEE, Chung-Chih Lei, and Siu-Wan Hung, "Computer-Aided Kidney Segmentation on Abdominal CT Images, "IEEE Transactions on Information Technology in Biomedicine,vol.10.no.1,Jan 2006.
[15]. W.L.Kang,Q.Q.Yang and R.R.LLiang," The Comparative Research on Image Segmentation Algorithm, "IEEE Conference,2009.
[16]. Zhang Y.J , "An overview of image and video segmentation in the last 40 year ",IEEE Conference ,pp.101-106,2009
[17]. V. K. Dehariya, S. K. Shrivastava, R. C. Jain,"Clustering of Image Data Set Using K-Means and Fuzzy K-Means Algorithms", International conference on CICN, pp. 386-391, 2010. [18] S. [20] Naz, H. Majeed, H. Irshad,"Image Segmentation using Fuzzy Clustering: A Survey", International Conference on ICET, pp.181-186, 2010.
[18]. Segmentation Techniques For Image Analysis IJAERS/Vol. I/ Issue II/January-March, 2012.
[19]. Qingsong Zhu and Zhansong,"ANovel Recurssive Learning-Based method for the efficient and accurate segmentation of video with Dynamic Background, "IEEE Transactions. Sep 2012.